STUDY ON HYDRODYNAMIC CHARACTERISTICS OF SWIRL BURNER BASED ON CFD

by

Xiaomin WU[a] and Li JIA[b*]

[a] School of Civil Affairs and Social Governance, Chongqing City Management College, Chongqing, China
[b] School of Intelligent Engineering, Chongqing City Management College, Chongqing, China

Original scientific paper
https://doi.org/10.2298/TSCI2203385W

The numerical simulation method is mostly used to analyze the gas-solid two-phase hydrodynamics of swirl burner, ignoring the simulation of boundary conditions of swirl burner, resulting in poor simulation effect. To solve this problem, a CFD based study on the hydrodynamic characteristics of swirl burner is proposed. The physical model of swirl burner is constructed by using FLUENT software. The particle concentration of the burner is calculated, and the Lagrange motion function of gas-solid two-phase flow is established to obtain the boundary conditions of the swirling burner and simulate the gas-solid two-phase flow. The motion equation of swirl burner is constructed, the dynamic characteristics are analyzed, and the dynamic equation is derived. The experimental results show that the swirl burner has less response and better performance under the impact of rolling direction.

Key words: *swirl burner, CFD, hydrodynamic characteristics, motion function, boundary condition*

Introduction

Gas turbine engines for power generation and propulsion applications traditionally use diffusion flame swirl burners [1], which have reliable performance and reasonable stability characteristics, such as gas turbines, presses and furnaces. The re-circulation zone generated by swirl or bluff body not only enhances the mixing of fuel and air, but also brings back hot combustion products to ignite reactants and stabilize the flame [2]. Therefore, the swirling combustion flame is stable, and in most cases, the re-circulation vortex shortens the length of the flame. With the development of combustion technology, the swirl combustion technology developed on this basis is widely used in engineering combustion. It mainly depends on the centrifugal effect and vortex effect of swirl to control reaction mixing and flame propagation. The basic principle is that the unburned gas mixture with high density moves from inside to outside under the pressure difference generated by strong centrifugal force, while the combusted material with low density moves from outside to inside to ignite the unburned gas mixture in the movement. In the swirl burner, the main function of swirl is to form a central reflux zone, realize flame stability, improve fuel mixing, improve combustion efficiency, and reduce pollutant emission a certain extent [3]. At medium and high swirling flow intensity, due to the generation of reflux zone, the stability of flame is increased, the ignition point is close to the nozzle, the expansion angle of jet is increased, the entrainment is increased, the mixing is more

* Corresponding author, e-mail: lijia_researcher@163.com

intense, the combustion intensity is higher, and a shorter and wider flame is formed. The central reflux zone can provide all conditions required for flame stability in high speed flow, keep the fuel for a long residence time, improve its mixing speed and reaction temperature, and improve its combustion efficiency [4]. Therefore, many burners use swirl to control mixing and flame structure. The annular re-circulation zone formed by swirling combustion in the combustion center is a good mixing zone for hot combustion products, which plays the role of storing heat and chemically active substances, so that heat and quality can be effectively transferred from combustion products to new combustible mixture through high turbulence, so as to fully burn the fuel [5]. Therefore, the re-circulation zone in the swirl burner due to strong fluid rotation plays an important role in stabilizing the flame.

Relevant scholars have put forward many studies on this. Qiang *et al*. [6] proposed the flame stability mechanism and shape transformation of 3-D printing methane-rich hydrogen/air low swirl burner, and studied the shape and transformation of premix methane-rich hydrogen flame in 3-D printing low swirl burner by using synchronous OH × CH_2O plane laser-induced fluorescence and 3-D particle image velocimetry technology. Three different flame shapes were observed, namely bowl shape, W-shape and crown shape. The bowl flame is stabilized at the bottom through the balance of flame velocity, and its side is stabilized in the internal shear layer. Although the bulge of W-shaped flame depends on a similar stability mechanism in the central flow, its outer edge is stabilized by large-scale vortices in the external shear layer. The crown flame also has aerodynamic stability in the center, but its outer edge is fixed on the burner hardware. Under fixed equivalence ratio, the statistical transformation between flame shapes under test conditions is determined by hydrogen content and volume velocity. Dynamically, the transition from W to crown is attributed to the upstream propagation and attachment of the outer edge of the flame. Skvorinskien *et al*. [7] the combustion of waste gas in low swirl burner under syngas and oxygen enrichment conditions, biogas production of biomethane may lead to the emission of waste gas into the atmosphere. Since these gases consist of up to 15% methane, they should be used on site to reduce the impact of climate change. However, due to the low calorific value, the combustion process of these gases may be complex or even impossible. Therefore, the complex measures affecting the flammability limit and effectiveness of combustion waste gas in the designed low swirl burner with different swirlers can be clarified. The blade angles of the cyclone are 37°, 45°, and 53°. The critical region of flame structure was experimentally studied by chemiluminescence method to determine the OH^* emission intensity under syngas and oxygen enrichment conditions. The results show that considering the stable flame and the lowest CO emission, the most suitable combustion conditions can be obtained by using the cyclone with blade angle of 45°. In addition, in the case of syngas concentration, when additional oxygen enriched air is provided, it is possible to achieve more stable combustion conditions in consideration of lower CO and NO_x emissions. Based on the previous research, a CFD based study on the hydrodynamic characteristics of swirl burner is proposed. Through computer numerical calculation and image display, the system containing relevant physical phenomena such as fluid-flow and heat conduction is analyzed. Its emergence marks a new stage in the development of engineering fluid mechanics. Its basic idea can be summarized replace the original continuous physical quantity fields in time domain and space domain, such as velocity field and pressure field, with a set of variable values on a series of finite discrete points, establish algebraic equations about the relationship between field variables at these discrete points through certain principles and methods, and then solve the algebraic equations to obtain the approximate values of field variables. The results show that the response of swirl burner under the impact of rolling direction is small, and the jump force value is higher than other methods.

Numerical simulations of gas-solid two-phase flow in swirl burner

Basic principle of numerical simulation of gas-solid two-phase flow

Before optimizing the current data simulation method, it is necessary to carry out a lot of preparatory work on the combustion technology of swirl burner and sort out the relevant principles of this research. This study will mainly use the improved model as the data calculation basis in numerical simulation. In the original numerical simulation calculation unit, the calculation coefficient X_d is revised. The coefficient correction process:

$$X_d = X_n \times (1 + R_i) \tag{1}$$

where R_i is the burner rotation coefficient in the calculation process, which can be expressed:

$$R_i = \frac{F_i}{E_i} \tag{2}$$

where F_i is the additional turbulent energy during burner rotation and E_i represents the value generated by the overall turbulent energy in the burner. Use the aforementioned equation to correct the calculation coefficient in the original numerical simulation model, and bring the corrected calculation results into the numerical simulation model as the numerical calculation part of this optimization process.

Construction of physical model of swirl burner

In order to ensure the accuracy of the numerical simulation process in this study, FLUENT software [8] is selected as the data simulation data calculation software, and the swirling burner data is introduced to build the swirling burner physical model. The construction steps of the physical model are shown in fig. 1.

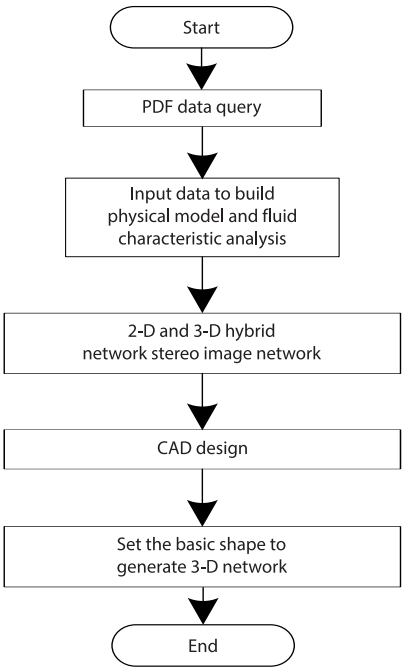

Figure 1. Flow chart of physical model construction of swirl burner

According to the contents in fig. 1, the 3-D model of swirl burner is constructed and meshed. All swirl burners adopt axial swirl straight blades. The blade thickness of the primary cyclone is 0.8 mm, the axial length of the blade is 6 mm and the number of blades is 12. The blade thickness of the secondary cyclone is 1.2 mm, the axial length of the blade is 10 mm, and the number of blades is 12. The fluid volume data and mixture data are used as the data sources during the construction of the physical model of the swirl burner [9]. Since these two parts of data contain a large amount of particle calculation, in order to ensure that the calculation results will not affect the subsequent numerical simulation, the particle loading rate is calculated:

$$\lambda = \frac{X_m P_m}{X_u P_u} \tag{3}$$

where it is represents the mass density of particle discrete phase. It represents the mass density of particle carrier phase and, respectively, represent two-phase particles. Use this part of data to build a 3-D motion model of substances in the burner. According to the use requirements of the burner [10], the unstructured network is used as the grid division calculation, the grid size is

set to 20 mm, and the number of grids is about 550000. The primary air inlet and secondary air inlet in the burner have a direct impact on the dynamic field of the burner. Therefore, the data in tab. 1 are used as the necessary data in the cyclone burner processing model.

Table 1. Physical model data of swirl burner

Project number	Project	Unit
1	Primary air inlet temperature	[℃]
2	Secondary air inlet temperature	[℃]
3	Air inlet temperature	[℃]
4	Primary wind speed	[ms^{-1}]
5	Secondary wind speed	[ms^{-1}]
6	Primary inlet blade angle	[°]
7	Secondary inlet blade angle	[°]
8	Rotating speed of primary inlet blade	[ms^{-1}]
9	Secondary inlet blade rotation speed	[ms^{-1}]

According to the contents in tab. 1, the physical model of burner is established by using Reynold's time average equation:

$$D_d = S_{\text{div}}(\alpha_i + \Delta i) + D_i \tag{4}$$

where S_{div} is the general variable in the physical model, α_i – the burner energy transfer coefficient, Δi – the flame retardant vector of the burner, and D_i – the original data item of the physical model. The equation is used to control the results of physical model construction. The physical model of swirl burner is characterized by strong adaptability and wide application. Firstly, the governing equations of general flow problems are non-linear, many independent variables, arbitrary geometry of calculation domain and complex boundary conditions. For these problems that cannot obtain analytical solutions, numerical solutions can well meet the needs of engineering. Secondly, various numerical experiments can be carried out by computer, and the calculation results can be improved through the selection of different parameters. It is not limited by the physical model, saving time, money and flexibility.

Analysis of gas-solid two-phase flow

Based on the physical model of swirl burner, the key data in gas-solid two-phase flow are obtained. The velocity field and concentration field of solid particles in the burner will be calculated to realize the direct simulation of gas-solid two-phase flow. According to the previous research requirements, the particle concentration in the burner will be calculated [11]. If the total amount of solid particles in the basic unit in the burner model is N_n:

$$N_n = \frac{\sum_m \sum_i (D_d E_m E_i)}{\Delta v} \tag{5}$$

where E_m and E_i is the residence time of particulate matter and Δv – the required velocity of particulate matter:

$$N_{nm} = \frac{N_n}{H_{ai}} \tag{6}$$

where H_{ai} is the flow of solid particles with an initial diameter of i moving along the a molecule. Using the aforementioned equation, the movement of particles in the burner can be analyzed

[12, 13]. In order to complete the numerical simulation of gas-solid two-phase flow, the particle momentum equation can be shown:

$$F_c = W_d + \frac{j_h(\rho_i - \rho)}{\rho_i} + W_h \tag{7}$$

where W_d is the gas phase resistance inside the burner, ρ_i – the actual density of particles inside the burner, ρ – the predicted density of particles inside the burner, j_h – the gravity of particles, and W_h – the force of other parts in the burner. The Lagrange motion function of particles can be obtained from this equation. This function is used as the basis of numerical simulation in the subsequent data simulation process.

Gas-solid two-phase numerical simulation

According to the aforementioned analysis of gas-solid two-phase flow, the gas-solid two-phase numerical simulation process is set as shown in fig. 2:

According to the preset improved model in this study, the burner rotating jet data are analyzed. According to the analysis results, the gas-flow rotation characteristics in the burner are obtained, which are combined with the analysis results of gas-solid two-phase flow and brought into the traditional numerical simulation method to complete the optimization process:

$$B = V_v T_t P_p F_c \tag{8}$$

$$S = V_v T_t P_p B \tag{9}$$

where V_v is the axial angular velocity on the jet section of the burner, T_t – the tangential time on the jet section, and P_p – the static force in the burner. Using the aforementioned equation to analyze the rotation of the air-flow in the burner, the force of particles on the gas in the burner is obtained:

$$F_l = \frac{\sum_{i=1}^{n} F_i}{\Delta v} BS \tag{10}$$

where F_i is the force of particles in the burner on the gas volume. In order to ensure the accuracy of numerical simulation, the burner numerical simulation boundary conditions are set [14]. The inlet boundary of gas-solid two-phase flow can be set into three parts, namely, the diameter of mixed phase particles, the inlet velocity of air phase and the inlet velocity of particle phase. The boundary conditions can be set:

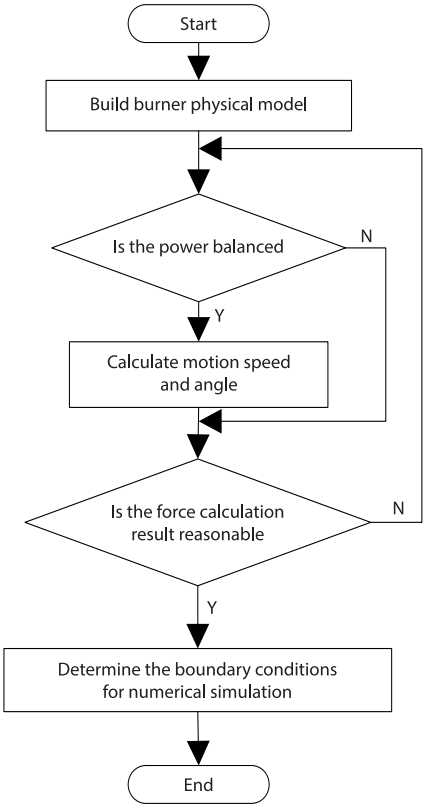

Figure 2. Gas-solid two-phase numerical simulation process

$$T_z = \frac{\rho_j v_j D}{\mu_j} F_l \tag{11}$$

where ρ_j is the particle diameter of the mixed phase, v_j – the air inlet velocity of the air phase, D – the particle diameter, and μ_j – the dynamic viscosity of the mixed phase. The calculation results of this equation are used to control the calculation process of the gas-solid two-phase

flow numerical simulation model. The previous contents are integrated and the optimization results are brought into the traditional numerical simulation method to complete the gas-solid two-phase flow in the swirl burner Numerical simulation design process of flow.

Hydrodynamic characteristics of swirl burner under CFD

Structural motion equation of swirl burner

Through the structural components of the swirl burner and according to the appropriate motion combination, the extension of the capture ring and the tension of the capture ring at the beginning, during and at the end of docking are completed, so as to ensure the flexible movement of the capture ring in the direction of 6-DoF during docking, provide convenience for capture connection, and then provide effective damping and buffer. The kinetic energy generated by contact and impact when the swirling burner structure realizes space docking.

– Spring mechanism

In the electromechanical machining system, a total of six spring mechanisms using plane volute spring are set, and J is set to represent the stiffness of the spring mechanism. There are two springs with different working forms in the swirl burner. One is the uniaxial bidirectional rotating spring J_1 installed at the lead screw assembly, the other is the biaxial bidirectional rotating springs J_2 and J_3 installed in front of the friction brake and connected to both ends of the differential. The S_1 and S_2 can be used to represent the stress and deformation of uniaxial bidirectional rotating spring and biaxial bidirectional rotating spring in swirl burner, respectively:

$$S_1 = \frac{1}{2} J \beta^2 \tag{12}$$

$$S_2 = \frac{1}{2} J (\beta_1 - \beta_2)^2 \tag{13}$$

where β, β_1, and β_2 are the rotation angle corresponding to the rotation axis.

– Electromagnetic brake

Electromagnetic brake is a damping element, which exists in the lead screw connection combination. When the speed of electromagnetic brake is not high, the rotor speed is actually directly proportional to the braking torque. When constructing the dynamic equation, the linear function of velocity can be used to replace the damping force of the brake, and the quadratic homogeneous function of velocity can be used to replace the dissipation function:

$$Z_z = \sum_{i=1}^{n} \sum_{j=1}^{n} W_{ij} w_i w_j \tag{14}$$

where n is the number of electromagnetic brakes in the lead screw connection combination, W_{ij} – the dissipation coefficient, and w_i, w_j are the Rayleigh dissipation function.

Analysis on hydrodynamic characteristics of swirl burner

Dynamic characteristic analysis

When the lead screw does not rotate around the axis, the relationship between the speed ω_1 of the lead screw and the speed v of the lead screw along the axis can be expressed:

$$X_z = \frac{Z_z M_t}{2\pi} \tag{15}$$

where M_t is the spiral lead.

According to the velocity synthesis theorem, the average velocity of the lead screw along the axis is the same as the projection corresponding to the motion velocity of any point on the lead screw axis. Assuming that there are upper hinge points and lower hinge points in the lead screw axis:

$$B_v = \dot{H}\cos\eta X_z \tag{16}$$

where η is the included angle between the axis of the swirl burner and the axis of the lead screw and H – the average moving speed corresponding to the distribution plane of the hinge points along the axis of the swirl burner.

Dynamic equation

Assuming that the axial force, F_x, acts on the swirl burner, the state of the friction brake is locked [15]. Let M is the mass of the fixed coupling member and the capture ring without considering the mass of other members. The following equation is obtained through the virtual power principle and the D'Alembert principle:

$$(F_x - \dot{H})\delta - T_B\delta B_v = 0 \tag{17}$$

where δ is the rigidity coefficient and T_B – the torque of the starting spring in the swirl burner. Let the starting spring T_g be a linear spring in the swirl burner, and its expression:

$$T_g = T_0 + C_S\theta \tag{18}$$

where C_S is the spring stiffness, T_0 – the spring preload torque, and θ – the maximum spring stiffness.

If the axial force, F_x, is continuously increased when the starting spring is at the limit stroke, the friction brake will slip. Assuming that the starting spring mechanism is transformed into a rigid transmission mechanism at this time, without considering the transmission inertia of the friction brake in the swirl burner, the variational form corresponding to the dynamic equation of the swirl burner is obtained. The motion of fluid is also governed by three physical conservation laws, namely, mass conservation, momentum conservation and energy conservation. The governing equations of fluid motion describe these conservation laws, including continuity equation reflect mass conservation, Navier-Stokes equation reflect momentum conservation and energy equation reflect energy conservation. If the flow contains the mixing or interaction of different components, the system should also abide by the law of component conservation. The main steps of calculating the hydrodynamics of swirl burner are shown in fig. 3.

As shown in fig. 3, the main steps of CFD are to simplify the physical model into a mathematical model according to the actual physical model, and select the corresponding closed control equations for different mathematical models. The governing equa-

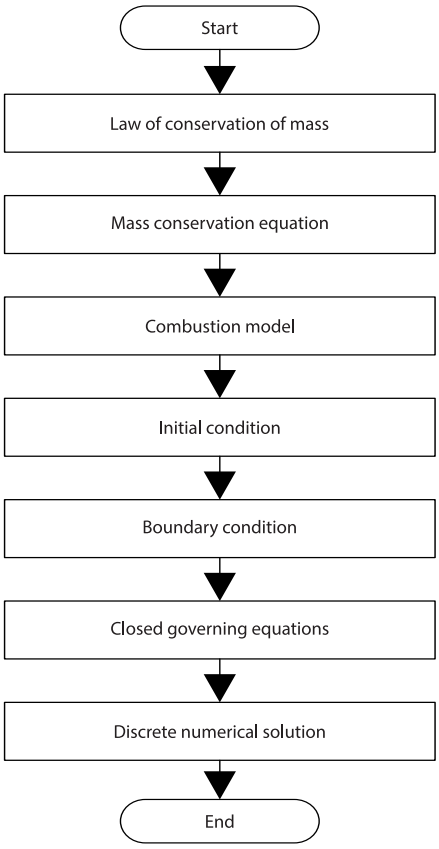

Figure 3. Main steps of CFD

tions are discretized to a series of grid nodes or grid centers by numerical methods such as finite volume method and finite element method, and the differential equations are transformed into algebraic equations. After many iterations, the stable and convergent discrete numerical solutions are obtained. For the combustion model, the main fuel flow is the rotating jet entering the combustion chamber through the cyclone in the premixed mode, and the duty fuel is the DC jet burning through the diffusion mode. The fuel on duty accounts for about 10% of the total fuel under rated thermal power. When selecting the model, the rotating jet characteristics of the main fuel jet are fully considered. The turbulence model used is the Reynolds stress model including seven equations, taking into account the anisotropy of vortices in all directions, so that the turbulence model applied to 3-D simulation, especially the 3-D simulation under the characteristics of swirling flow, is closer to the real situation. As for the combustion model, because various vortices in the combustion chamber have a great impact on the mixing process of unburned mixture and flammable mixture in the swirling combustion process, the combustion process in the swirling combustion process is mainly affected by the turbulent dissipation process. According to the conclusion of Dam Kohler number, when the chemical reaction time is far less than the turbulent diffusion time. It can be assumed that the chemical reaction in the flow field is nearly infinitely fast. Therefore, considering all factors, the combustion model is selected, so as to complete the research on the hydrodynamic characteristics of Swirl Burner Based on CFD.

Experimental analyses

In this study, the hydrodynamic characteristics of Swirl Burner Based on CFD are proposed. In order to verify the application effect of the research content, the hydrodynamic characteristics of swirl burner are analyzed according to the obtained dynamic characteristic equation, and the kinematic response of swirl burner is obtained. The experimental duration is one month. The experimental parameters such as the displacement response corresponding to the angular displacement of the capture ring of the swirl burner and the constraint response of the screw hinge under step impact are obtained. The simulation software is MATLAB7.0 software, the operating system is WINDOWS10, and the memory is 24 GB. The structural parameters of the experimental swirl burner are set, as shown in tab. 2.

Table 2. Structural parameters of swirl burner

Serial number	Parameter name	Specific value
1	Theoretical air volume [Nm^3kg^{-1}]	6.20
2	Calculation of coal consumption [kgh^{-1}]	242153.5
3	Initial drying dose [kg]	2.05
4	Air leakage rate [%]	0.07
5	Central wind rate [%]	0
6	Outer diameter of center tube [m]	0.55
7	Center tube thickness [m]	0.02
8	Sectional area of primary air outlet [m^2]	0.30
9	Sectional area of secondary air outlet [m^2]	0.25
10	Number of operating burners (Platform)	1

The data in tab. 2 are the measured data of swirl burner, which are input into the simulation software to build the 3-D model of swirl burner. The gas-solid two-phase flow in

the aforementioned swirl burner is numerically simulated by using the method in this paper, the method in [6] and the method in [7], and the differences of the three methods are compared.

When coaxially tensioned or coaxially pushed out, the function of swirl burner requires that all screw members bear uniform force in the burner. The stress of each screw member when the swirl burner is connected with the gear, the spring shaft is locked and pushed out coaxially is shown in fig. 4.

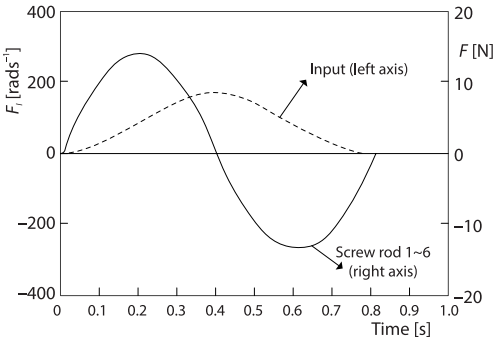

Figure 4. Stress of each screw member

According to the analysis of fig. 4, the working change curves of different screw rods are completely coincident, indicating that under this working condition, the force of each screw rod in the swirl burner is uniform, and the buffer damping of the swirl burner meets the requirements of special functions.

Under the influence of the impact force in the rolling direction, the displacement response curve corresponding to the angular displacement of the capture ring in the swirl burner is shown in fig. 5.

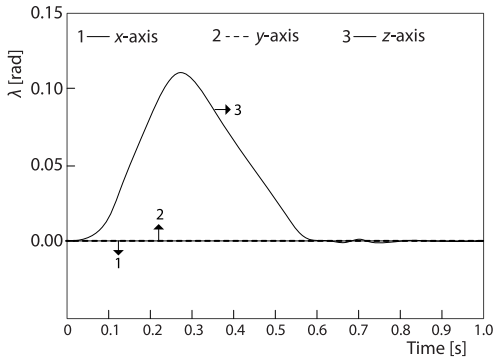

Figure 5. Response curve corresponding to capture ring displacement

By analyzing fig. 5, it can be seen that the angular displacement of the capture ring is zero in both the *x*-axis direction and the *y*-axis direction, and there is only the angular displacement obtained by capturing around the *z*-axis. Through the aforementioned analysis, it can be seen that the motion response characteristics of the capture ring are pure rolling in the swirl burner, and there is usually a very small linear displacement in the *z*-axis direction. Through further analysis and calculation, it can be seen that the two screw rods in the same screw rod group have different stress conditions in the swirl burner, but the components in different screw rod groups have the same stress response, indicating that the swirl burner has less response under the impact of rolling direction.

When calculating and analyzing the buffer damping dynamic performance of the swirl burner, the corresponding ADAMS simulation model of the swirl burner is constructed to verify the step strength of the analysis results of the buffer damping dynamic performance analysis method of the swirl burner. The expression of the step strength function $F(t)$:

$$F(t) = \text{step}(t_1) - \text{step}(t_2) \tag{19}$$

where step() is the step function corresponding to the first derivative, t_1 – the initial response parameter of the binding force of the screw hinge, and t_2 – the initial response parameter of the capture ring angular displacement. The step forces of different methods are calculated through the previous equation, and the comparison results are shown in fig. 6.

According to fig. 6, compared with other methods, the step force value of CFD based swirl burner hydrodynamic characteristic method is higher, while the literature method is relatively low. The reason is that under different conditions, the system plays a buffer and attenuation role under the force of different screw rods in the swirl burner and the action of external

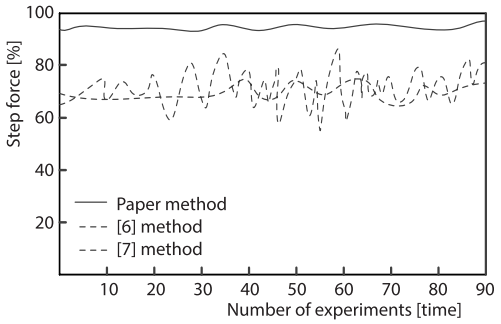

Figure 6. Step strength comparison results of different methods

energy. On the premise of reasonable parameter matching, the swirl burner can effectively dissipate and absorb the action energy in the 6-DoF directions of space, which is conducive to improving the step strength to a certain extent.

Conclusions

- Based on the hydrodynamic characteristics of the swirl burner based on CFD, the force of each screw in the swirl burner is uniform, and the buffer damping of the swirl burner meets the requirements of special functions.
- The two screw rods in the same screw rod group have different stress conditions in the swirl burner, but the components in different screw rod groups have the same stress response, indicating that the response of the swirl burner under the impact of rolling direction is small.
- The step force value of the CFD based method for the hydrodynamic characteristics of swirl burner is higher than that of other methods.

Prospects

- Based on the hydrodynamic characteristics of the swirl burner based on CFD, the force of each screw in the swirl burner is uniform, and the buffer damping of the swirl burner meets the requirements of special functions.
- The two screw rods in the same screw rod group have different stress conditions in the swirl burner, but the components in different screw rod groups have the same stress response, indicating that the response of the swirl burner under the impact of rolling direction is small.
- The step force value of the CFD based method for the hydrodynamic characteristics of swirl burner is higher than that of other methods.

Acknowledgment

The research is supported by: Chongqing Municipal Education Commission of Science and Technology Research Project, Study on progressive damage and permeability enhancement mechanism of coal seam hydraulic fracturing and optimization of extractable range (No. KJQN202003302); Chongqing Municipal Education Commission of Science and Technology Research Project, The study on the Mechanism and the Rule of Migration and Transformation about Organic Components in Pretreatment-Anaerobic Digestion (No. KJQN202103303); Chongqing Municipal Education Commission of Science and Technology Research Project, Non-linear macro meso mechanical response mechanism of bulk gangue (No. KJQN201903313); The 3rd Batch Innovation Team Project of Chongqing City Management College, Gangue Resource Utilization and Mechanical Research and Analysis (No. KYTD202003); The 4rd Batch Innovation Team Project of Chongqing City Management College. Water Environment Treatment and Resource Utilization (No. KYTD202101).

References

[1] Shp, A., *et al*., A Comparative Exploration of Thermal, Radiative and Pollutant Emission Characteristics of Oil Burner Flame Using Palm Oil Biodiesel-Diesel Blend Fuel and Diesel Fuel, *Energy*, *15* (2020), 119338

[2] Rva, A., *et al*., Assessment of Laminar Flame Velocity of Producer Gas from Biomass Gasification Using the Bunsen Burner Method, *International Journal of Hydrogen Energy*, *45* (2020), 20, pp. 11559-11568
[3] Hidegh, G., *et al*., Distributed Combustion of Diesel-Butanol Fuel Blends in a Mixture Temperature-Controlled Burner, *Fuel*, *307* (2022), 1, 121840
[4] Ilbas, M., *et al*., Oxidizer Effects on Ammonia Combustion Using a Generated Non-Premixed Burner, *International Journal of Hydrogen Energy*, *12* (2021), 6, pp. 1-10
[5] Ma, X., *et al*., Evaluation and Characterization of a Durable Composite Phase Thermal Barrier Coating in Solid Particle Erosion and Burner Rig Tests, *Journal of Thermal Spray Technology*, *30* (2020), 7, pp. 69-80
[6] Qiang, A., *et a*l., Flame Stabilization Mechanisms and Shape Transitions in a 3-D Printed, Hydrogen Enriched, Methane/Air Low-Swirl Burner, *International Journal of Hydrogen Energy*, *194* (2021), pp. 14764-14779
[7] Skvorinskien, R., *et al*., Combustion of Waste Gas in a Low-Swirl Burner under Syngas and Oxygen Enrichment, *Fuel*, *298* (2021), 2, 120730
[8] Oh, D. H., *et al*., Software Platform for Computation Fluid Dynamics Simulation of Mixing and Crystallization in a Stirred Vessel, *Crystal Growth & Design*, *20* (2019), 2, pp. 1172-1185
[9] Lopez-Ruiz, G., Experimental and Numerical Study of NO Formation in a Domestic H2/Air Coaxial Burner at Low Reynolds Number, *Energy*, *221* (2021), 3, 119768
[10] Agwu, O., *et al*., Flame Characteristics of Glycerol/Methanol Blends in a Swirl-Stabilised Gas Turbine Burner, *Fuel*, *290* (2021), 5, 119968
[11] Skvorinskien, R., *et al*., Combustion of Waste Gas in a Low-Swirl Burner under Syngas and Oxygen Enrichment, *Fuel*, *298* (2021), 2, 120730
[12] Chand, S., Influence of B4C/BN on Solid Particle Erosion of Al6061 Metal Matrix Hybrid Composites Fabricated through Powder Metallurgy Technique, *Ceramics International*, *46* (2020), 11, pp. 17621-17630
[13] Arani, N. H., *et al*., Modelling the Solid Particle Erosion of Rubber Particulate-Reinforced Epoxy, *Tribology International*, *153* (2021), 1, 106656
[14] Jeon, J., Spatiotemporal Flame Propagations, Combustion and Solid Particle Emissions from Lean and Stoichiometric Gasoline Direct Injection Engine Operation, *Energy*, *210* (2020), 11, 118652
[15] Geng, K. H., *et al*., Thermal Jitter Optimization Analysis of Ventilated Disc Brake, Computer Simulation, *36* (2019), 9, pp. 156-160

Paper submitted: September 30, 2021
Paper revised: December 4, 2021
Paper accepted: February 7, 2022